

Collimator Study of a Pre-Clinical Pixelated Semiconductor SPECT System using Monte Carlo Simulation

Hyun-Woo Jeong, Jong Seok Kim, Se Young Bae, Kanghyen Seo, Seung Hun Kim, Seong Hyeon Kang, Dong Jin Shin, Kyuseok Kim, and Youngjin Lee

Abstract—In single photon emission computed tomography (SPECT) with pixelated semiconductor detector (PSD), not only pinhole collimator but also parallel-hole collimator is often used in pre-clinical nuclear medicine imaging system. The purpose of this study was to evaluate and compare pinhole and parallel-hole collimators in PSD. In this study, we performed a simulation study of the PID 350 (Ajat Oy Ltd., Finland) CdTe PSD using a Geant4 Application for Tomographic Emission (GATE) simulation. For that purpose, we designed four collimators which are most frequently used in the pre-clinical nuclear medicine: (1) pinhole collimator, (2) low energy high resolution (LEHR), (3) low energy general purpose (LEGP), and (4) low energy high sensitivity (LEHS) parallel-hole collimator. The sensitivity and spatial resolution of the four collimators were evaluated using point source. Moreover, to assess the overall performance of the imaging system, a hot-rod phantom was designed using a GATE simulation. The highest sensitivity was achieved using LEHS, followed by LEGP, LEHR, and pinhole. Also, at 2 cm source-to-collimator distance, the spatial resolution was 1.63, 2.05, 2.79, and 3.45 mm using pinhole, LEHR, LEGP, and LEHS, respectively. The reconstructed hot-rod phantom images showed that the pinhole collimator and the LEHR parallel-hole collimator give a fine spatial resolution for pre-clinical SPECT with PSD. In conclusion, we successfully compared different types of collimator with pre-clinical pixelated semiconductor SPECT system.

Youngjin Lee, Prof., is with the Department of Radiological Science, Eulji University, 553, Sanseong-daero, Seongnam-si, Gyeonggi-do, Korea (corresponding author to provide phone: +82-31-740-7264; fax: +82-31-740-7351; e-mail: radioyoungj@gmail.com).

Hyun-Woo Jeong, Prof., is with the Department of Biomedical Engineering, Eulji University, 553, Sanseong-daero, Seongnam-si, Gyeonggi-do, Korea (e-mail: skyjhw99@gmail.com).

Jong Seok Kim is with the Department of Radiological Science, Eulji University, 553, Sanseong-daero, Seongnam-si, Gyeonggi-do, Korea (e-mail: js2good@naver.com).

Se Young Bae is with the Department of Radiological Science, Eulji University, 553, Sanseong-daero, Seongnam-si, Gyeonggi-do, Korea (e-mail: seyoung0902@naver.com).

Kanghyen Seo is with the Department of Radiological Science, Eulji University, 553, Sanseong-daero, Seongnam-si, Gyeonggi-do, Korea (e-mail: lirkgusil@naver.com).

Seung Hun Kim is with the Department of Radiological Science, Eulji University, 553, Sanseong-daero, Seongnam-si, Gyeonggi-do, Korea (e-mail: in-boy@hanmail.net).

Seong Hyeon Kang, is with the Department of Radiological Science, Eulji University, 553, Sanseong-daero, Seongnam-si, Gyeonggi-do, Korea (e-mail: tjdgus7345@nate.com).

Dong Jin Shin is with the Department of Radiological Science, Eulji University, 553, Sanseong-daero, Seongnam-si, Gyeonggi-do, Korea (e-mail: ddongjy12@naver.com).

Kyuseok Kim is with the Department of Radiological Science and Convergence Engineering, Yonsei University, 1, Yonsei-dae-gil, Wonju-si, Korea (e-mail: seokkyu502@yonsei.ac.kr).

Keywords—Nuclear medicine imaging, Single photon emission computed tomography (SPECT), Pixelated semiconductor, Collimator, Monte Carlo simulation.

I. INTRODUCTION

CONVENTIONAL single photon emission computed tomography (SPECT) system is most often based on the Anger camera principle using a collimator placed in front of a NaI(Tl) or CsI(Tl) scintillation crystal [1]. However, the intrinsic resolution of a scintillation detector is relatively low (approximately 3.0 - 4.0 mm full width at half maximum (FWHM)) [2]. One strategy to cope with low intrinsic resolution is to use pixelated semiconductor detectors (PSD) using cadmium telluride (CdTe) or cadmium zinc telluride (CZT) [3]-[7]. The intrinsic resolution of PSD is almost equal to the pixel size because the carriers are collected individually for each pixel with directly convert gamma ray photons into electrons [4].

In SPECT, the collimator is essential component of the system because the image performance such as sensitivity and spatial resolution is mainly dependent on the collimator [8]. Collimators are generally classified as parallel-hole, pinhole, converging, and diverging types. Almost all pre-clinical SPECT system is performed with pinhole collimator and parallel-hole collimator. Pinhole collimator has been widely used for pre-clinical SPECT system because of their excellent spatial resolution [9]-[11]. Also, pinhole collimator can be very useful in pre-clinical research where small organ such as thyroid or parathyroid is usually imaged as a target [12], [13]. Also, nearly all pre-clinical SPECT system uses parallel-hole collimator as the image-forming aperture. Parallel-hole collimators are generally desirable for most all nuclear medicine imaging applications due to the optimum image performance offered by such a dense arrangement of aperture. Although we have to select collimator to obtain appropriate image performance and accurate analysis results, there have been no comparative studies on image performance with various collimators in pre-clinical pixelated semiconductor SPECT system. So, we compared the image performances of pinhole and three types of parallel-hole collimators (low energy high resolution (LEHR), low energy general purpose (LEGP), and low energy high sensitivity (LEHS)) in pre-clinical pixelated semiconductor SPECT system using a GEANT4 Application for Tomographic Emission (GATE)

simulation in this study.

The collimators were simulated with a PID 350 (Ajat Oy Ltd., Finland) CdTe PSD using a GATE. The sensitivity and spatial resolution were evaluated for each source-to-collimator distance. To evaluate the overall image performance, a hot-rod phantom was designed using GATE. The simulated comparison results obtained for various collimators are presented and discussed.

II. MATERIALS AND METHODS

A. Monte Carlo simulation

GATE is a widely used Monte Carlo simulation platform with general purpose code Geant4 and an advanced open source software developed by the international OpenGATE collaboration in 2001 [14]. The accuracy, usefulness and effectiveness of this platform have been confirmed in many studies [14]-[17]. In this study, we used GATE version 6.

B. PID 350 CdTe PSD

Among available semiconductor detectors, single chemical element, such as silicon (Si) or germanium (Ge) detectors, is most frequently used in field of the nuclear medicine [18], [19]. However, the low atomic number of Si leads to the low absorption efficiency due to low stopping power for high energy gamma ray photons and Ge has major limitation such as narrow band-gap energy which only can be used at cryogenic temperature [20], [21]. Consequently, many studies have been conducted using pixelated semiconductor materials with wide band-gap such as CdTe in field of the nuclear medicine. CdTe pixelated semiconductor materials have been studied for their applications in nuclear medicine imaging. The useful properties of CdTe include its wide band gap, high atomic number, and good charge transport [22]-[24].

We modeled as the PID 350 CdTe PSD geometry using the tool within the GATE simulation. Pixel size of the PID 350 CdTe PSD was $0.35 \times 0.35 \text{ mm}^2$ with 128×128 pixels. The detector thickness was 1 mm and the physical gap was 1 pixel.

Fig. 1 shows the mass attenuation coefficients for various detector materials. As shown in Fig. 1, mass attenuation coefficient of CdTe is higher than other materials.

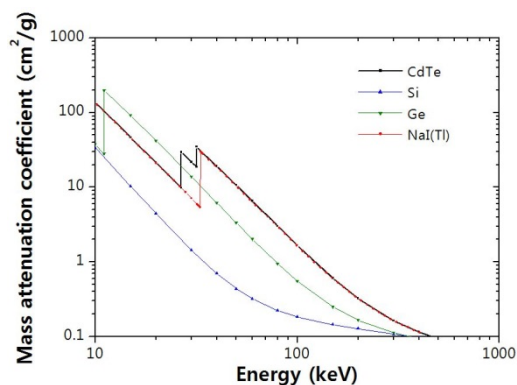


Fig. 1. Mass attenuation coefficients for CdTe pixelated semiconductor, Si semiconductor, Ge semiconductor, and NaI(Tl)

scintillation materials.

The efficiencies of the CZT pixelated semiconductor, Si semiconductor, Ge semiconductor, and NaI(Tl) scintillation detector as a function of thickness are shown in Fig. 2. Fig. 3 shows the efficiency of the 1 mm thickness above-mentioned detectors. The CdTe PSD had 32% efficiency at a 140 keV gamma ray energy.

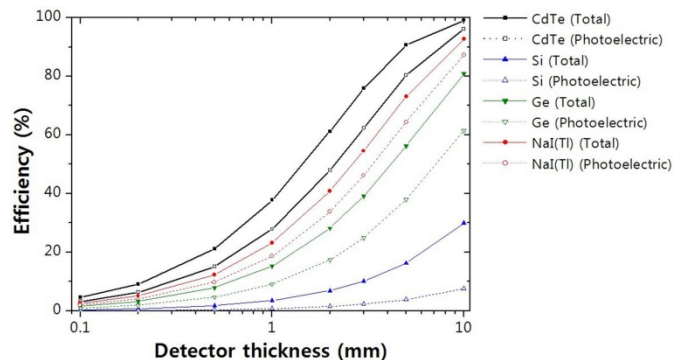


Fig. 2. The efficiency for 140 keV gamma ray energy for CdTe pixelated semiconductor, Si semiconductor, Ge semiconductor, and NaI(Tl) scintillation with respect to the detector thickness. Shown are the results for the total (solid lines) and photoelectric (dashed lines) efficiency.

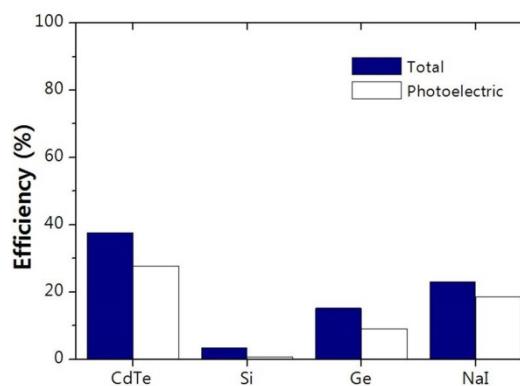


Fig. 3. The efficiency of a 1 mm thickness CdTe pixelated semiconductor, Si semiconductor, Ge semiconductor, and NaI(Tl) scintillation detector at a 140 keV gamma ray energy. The efficiency of the CdTe at a 1 mm thickness was 15.34, 2.69, and 1.56 times higher than that of Si, Ge, and NaI(Tl), respectively.

C. Pinhole and three parallel-hole collimators

We designed the four pre-clinical collimators: pinhole, LEHR parallel-hole, LEGP parallel-hole, and LEHS parallel-hole collimators. A previous paper demonstrated that the reconstructed hot-rod phantom images using most frequently used collimator materials (lead, tungsten, gold, and depleted uranium) were difficult to distinguish accurately (5). Based on this result, tungsten offers spatial resolution similar to those of the much more expensive gold and depleted uranium. Thus, we considered as tungsten collimator material in this study. Fig. 4 shows the cross-sectional views for the pinhole and parallel-hole collimators.

In pinhole collimator system, the efficiency ($\epsilon_{\text{pinhole}}$) and

resolution ($R_{pinhole}$) of the collimator was defined as follows [12]:

$$\epsilon_{pinhole} = \frac{a_{effective_efficiency}^2 \cos^3 \theta}{16b_{pinhole}^2}$$

$$(\quad a_{effective_efficiency} = \sqrt{a \left[a + \frac{2}{\mu} \tan^2 \left(\frac{\alpha}{2} \right) \right]} \quad)$$

(1)

$$R_{pinhole} = \frac{a_{effective_resolution} (l + b_{pinhole})}{l}$$

$$(\quad a_{effective_resolution} = a + \frac{\ln(2)}{\mu} \tan^2 \left(\frac{\alpha}{2} \right) \quad)$$

(2)

here $a_{effective_efficiency}$ is the effective pinhole diameter for sensitivity, θ is the angle between the source and detector center line, $b_{pinhole}$ is the source-to-pinhole collimator distance, a is the pinhole diameter, μ is the linear attenuation coefficient, α is the aperture angle of the pinhole collimator, $a_{effective_resolution}$ is the effective pinhole diameter for resolution, and l is the distance from the pinhole aperture to the detector surface. We designed the pinhole collimator by using a GATE simulation. The aperture angle was 50° , and the hole size of the pinhole collimator was 1.2 mm in diameter. In this study, the magnification factor of the pinhole collimator was 3.0 due to the ratios of the distances among the source, collimator and detector.

In parallel-hole collimator system, the efficiency ($\epsilon_{parallel-hole}$) and resolution ($R_{parallel-hole}$) of the collimator was defined as follows [2], [8]:

$$\epsilon_{parallel-hole} = K^2 \left(\frac{d}{h_{effective}} \right)^2 \frac{d^2}{(d+t)^2}$$

$$(\quad h_{effective} = h - 2\mu^{-1} \quad)$$

(3)

$$R_{parallel-hole} = d \frac{h_{effective} + b_{parallel-hole}}{h_{effective}}$$

(4)

where K is the constant that depends on the hole shape, d is the parallel-hole diameter, t is the septal thickness, $h_{effective}$ is the effective length of the parallel-hole collimator, h is the length of the parallel-hole collimator, and $b_{parallel-hole}$ is the source-to-parallel-hole collimator distance. We also designed the three type parallel-hole collimators (LEHR, LEGP, and LEHS parallel-hole collimators) by using a GATE simulation. The specifications of these parallel-hole collimators are shown in Table 1.

Table 1. The specifications of the parallel-hole collimators.

	LEHR	LEGP	LEHS
Hole diameter (mm)	1.2	1.6	2

Length (mm)	30	25.4	25.4
Septal thickness (mm)	0.2	0.25	0.3

D. Evaluation of image performance

To compare and evaluate the performance of the gamma camera systems, we evaluated both the sensitivity and spatial resolution. We used a ^{99m}Tc point source with an activity of 1 MBq with a 900 second scan time. Energy discrimination was applied to the 20% symmetrical energy window. The number of projections was 90 over 360° , and the data acquisition time was 10 second/view. The image reconstruction was carried out the ordered subsets-expectation maximization (OSEM) method. We used four subsets with five iterations. Evaluated sensitivity was represented in counts per second per kBq (cps/kBq). The spatial resolution was presented by the FWHM using a point spread function (PSF) in air.

To reduce statistical errors, ten simulations were performed for each source-to-collimator distance. Standard deviation (σ) was calculated as follows:

$$\sigma = \sqrt{\frac{\sum_{i=1}^n (N_i - \bar{N})^2}{(n-1)}} \quad (5)$$

where n is the number of measurements taken ($n = 10$), N_i is the datum from each measurement, and \bar{N} is the measured average of the data.

Finally, to evaluate overall image performance, hot-rod phantom images were generated in GATE simulation. It consisted of seven areas with rods of varying diameters that can be filled with activity. This phantom was filled with a water solution of ^{99m}Tc . Fig. 5 shows the hot-rod phantom diagram.

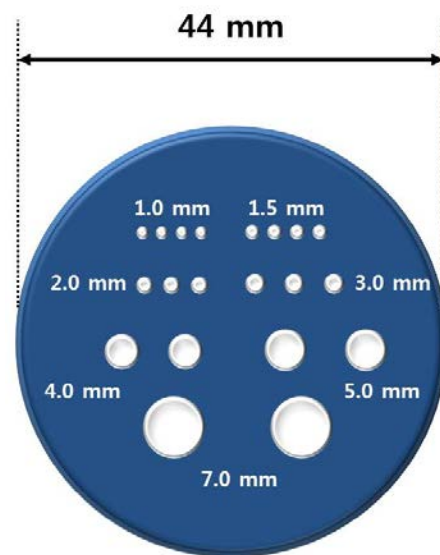


Fig. 5. Hot-rod phantom diagram. This phantom consisted of seven areas with rods of varying diameters (1.0, 1.5, 2.0, 3.0, 4.0, 5.0, and 7.0 mm) that can be filled with activity. Activities were

30,000, 55,000, 90,000, 135,000, 180,000, 280,000, and 445,000 Bq, respectively.

The distances between the point source or hot-rod phantom and collimator were 1, 2, 3, 4, and 5 cm for pre-clinical imaging.

III. RESULTS AND DISCUSSION

The sensitivities of the parallel-hole collimator are independent of the distance of the object from the collimator in all cases. The evaluated averages of the sensitivity for each source-to-collimator distance are shown in Fig. 6. A comparison of the sensitivities with respect to four types of collimator is shown in Fig. 7. The evaluated averages of the sensitivity for the LEHR, LEGP, and LEHS parallel-hole collimator are 0.09247, 0.23441, and 0.36773 cps/kBq, respectively. The sensitivity goes from pinhole, via LEHR parallel-hole and LEGP parallel-hole, to LEHS parallel-hole collimator in increasing order. In addition, the sensitivity for the pinhole collimator at 2 cm source-to-collimator distance is 0.00393 cps/kBq. When we compared the LEHS parallel-hole collimator and other collimators, the sensitivity of the LEHS was 3.98, 1.57, and 93.57 times higher than that of LEHR, LEGP, and pinhole, respectively.

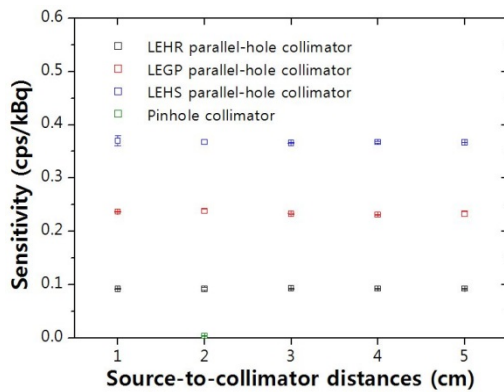


Fig. 6. Simulation results for the sensitivity with respect to the source-to-collimator distance for pinhole collimator and three parallel-hole collimators.

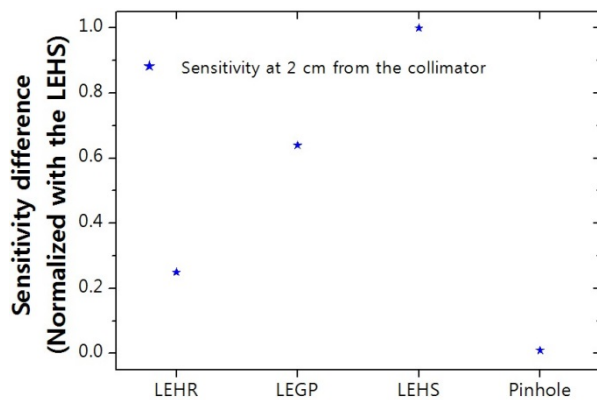


Fig. 7. Comparison of the simulation results for the sensitivity at 2 cm source-to-collimator distance. The results are normalized with

respect to the sensitivity obtained with a LEHS parallel-hole collimator.

The spatial resolutions of the parallel-hole collimator decrease with increasing distance from the collimator. Thus, the spatial resolution will be best for the object that is closest to the parallel-hole collimator in all cases. The evaluated averages of the spatial resolution for each source-to-collimator distance are shown in Fig. 8. A comparison of the spatial resolutions with respect to four types of collimator is shown in Fig. 9. At 2 cm source-to-collimator distance, the spatial resolution goes from pinhole, via LEHR parallel-hole and LEGP parallel-hole, to LEHS parallel-hole collimator in increasing order. According to the results, the average spatial resolution using the pinhole collimator was 20.49, 41.58, and 52.75% better than that attained with LEHR, LEGP, and LEHS parallel-hole collimator, respectively. In our system, the spatial resolution of images with pinhole collimator and LEHR parallel-hole collimator was 2.0 mm or less at 2 cm source-to-collimator distance, while other parallel-hole collimator provided about 3.0 mm.

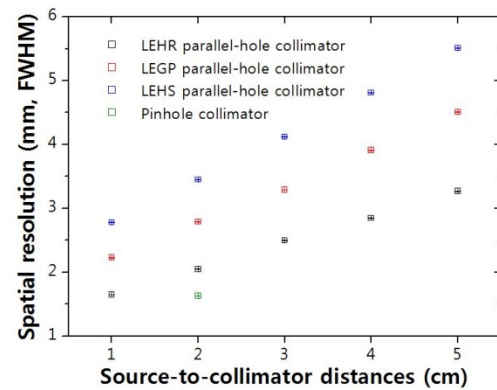


Fig. 8. Simulation results for the sensitivity with respect to the source-to-collimator distance for pinhole collimator and three parallel-hole collimators.

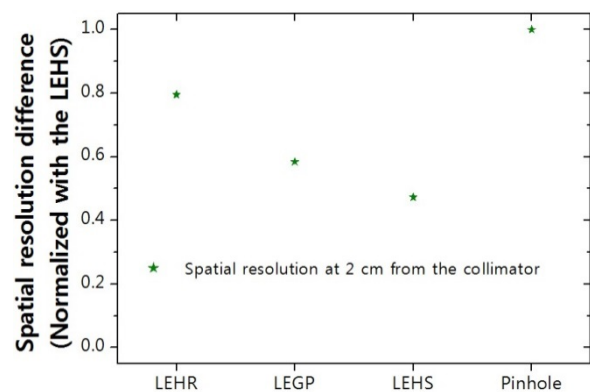


Fig. 9. Simulation results for the sensitivity with respect to the source-to-collimator distance for pinhole collimator and three parallel-hole collimators.

Finally, reconstructed images of the simulated hot-rod phantoms for each source-to-collimator distance are shown in

Fig. 10. The 2.0 mm rods were clearly resolved using LEHR parallel-hole collimator at 1 and 2 cm from the collimator and using pinhole collimator. Additionally, overall image performances in reconstructed hot-rod phantom images were in close agreement with the measured averages of spatial resolution results.

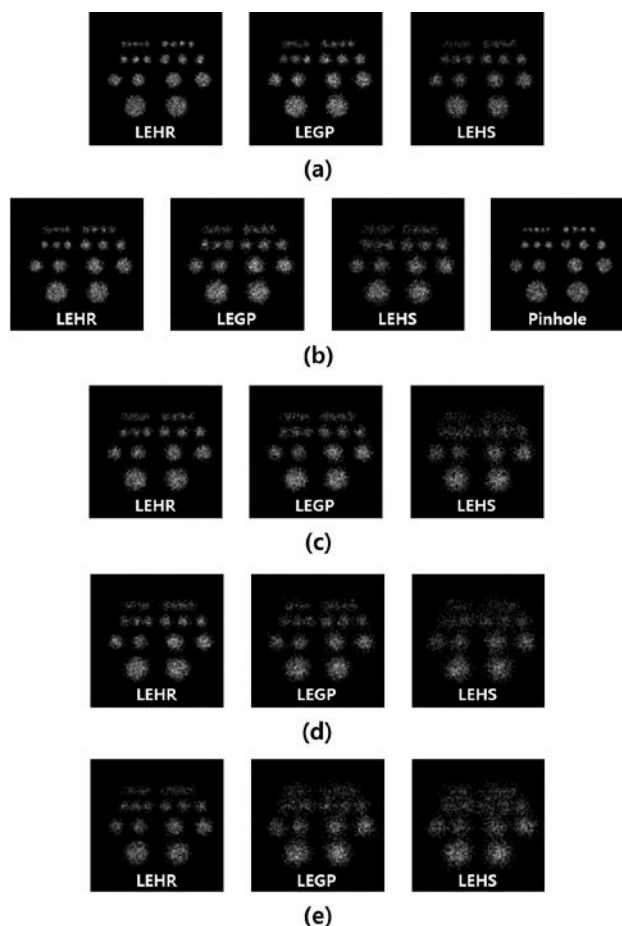


Fig. 10. Reconstructed images of the hot-rod phantom for pinhole collimator and three parallel-hole collimators for (a) 1 cm, (b) 2 cm, (c) 3 cm, (d) 4 cm, and (e) 5 cm source-to-collimator distance.

Image performances, such as sensitivity and spatial resolution, are determined by relationship between the direction of the detection point and the emitted gamma ray [25]. For a given total irradiation time, high sensitivity collimator, such as LEHS parallel-hole collimator, can acquire more counts because this collimator has wide collimator hole. However, it is increasingly realized that the quality of the counts is important, so the recommendation is generally against the utilization of high sensitivity collimator in this situation. Thus, choice is high resolution collimators, such as LEHR parallel-hole or pinhole collimators, in against the utilization of high sensitivity collimator. The utilization of high resolution collimators was recommended for gamma camera system, unless conditions suggest that unacceptably low count levels would occur. Consequently, trade-off between sensitivity and spatial resolution remains

fundamental consideration for types of collimator to obtain optimum image performances. Especially, the results in this study will be greatly helpful for choice of collimator in various situations.

IV. CONCLUSION

In the field of the nuclear medicine, we recommend applying a PSD to improve both the sensitivity and spatial resolution. A collimator study with a pre-clinical PSD by means of GATE simulation has been performed. We have presented comparison results for pinhole, LEHR parallel-hole, LEGP parallel-hole, and LEHS parallel-hole collimators with pre-clinical pixelated semiconductor SPECT system. We also evaluated and compared the above-mentioned collimators.

This study offered information for the utilization of appropriate collimators for various purposes. According to the results, although the parallel-hole collimators are often used in pre-clinical imaging, pinhole collimator should be used to obtain high spatial resolution images. Based on these results, we have to consider types of collimator to obtain higher performance of the imaging system.

REFERENCES

- [1] H. O. Anger, "Scintillation camera with multichannel collimators," *J. Nucl. Med.*, vol. 5, pp. 515-531, 1964.
- [2] H. Wiczorek and A. Goedicke, "Analytical model for SPECT detector concepts," *IEEE Trans. Nucl. Sci.*, vol. 53, pp. 1102-1112, 2006.
- [3] C. Scheiber and G. C. Giakos, "Medical applications of CdTe and CdZnTe detectors," *Nucl. Instrum. Meth. Phys. Res.*, vol. 458, pp. 12-25, 2001.
- [4] Y.-J. Lee, S.-J. Park, S.-W. Lee, D.-H. Kim, Y.-S. Kim, and H.-J. Kim, "Comparison of photon counting and conventional scintillation detectors in a pinhole SPECT system for small animal imaging: Monte Carlo simulation studies," *J. Kor. Phys. Soc.*, vol. 62, pp. 1317-1322, 2013.
- [5] Y.-J. Lee, H.-J. Ryu, S.-W. Lee, S.-J. Park, and H.-J. Kim, "Comparison of ultra-high-resolution parallel-hole collimator materials based on the CdTe pixelated semiconductor SPECT system," *Nucl. Instrum. Meth. Phys. Res.*, vol. 713, pp. 33-39, 2013.
- [6] T. Onodera, K. Hitomi, T. Shoji, and Y. Hiratake, "Pixelated thallium bromide detectors for gamma-ray spectroscopy and imaging," *Nucl. Instrum. Meth. Phys. Res.*, vol. 525, pp.199-204, 2004.
- [7] T. E. Peterson and L. R. Furenlid, "SPECT detectors: the Anger camera and beyond," *Phys. Med. Biol.*, vol. 56, pp. R145-R182, 2011.
- [8] S. C. Moore, K. Kouris, and I. Cullum, "Collimator design for single photon emission tomography," *Eur. J. Nucl. Med.*, vol. 19, pp. 138-150, 1992.
- [9] K. Ishizu, T. Mukai, Y. Yonekura, M. Pagani, T. Fujita, Y. Magata, S. Nishizawa, N. Tamaki, H. Shibasaki, and J. Konishi, "Ultra-high resolution SPECT system using four pinhole collimators for small animal studies," *J. Nucl. Med.*, vol. 36, pp. 2282-2287, 1995.
- [10] F. J. Beekman and B. Vastenhout, "Design and simulation of a high-resolution stationary SPECT system for small animals," *Phys. Med. Biol.*, vol. 49, pp. 4579-4592, 2004.
- [11] H. Iida and K. Ogawa, "Comparison of a pixelated semiconductor detector and a non-pixelated scintillation detector in pinhole SPECT system for small animal study," *Ann. Nucl. Med.*, vol. 25, pp. 143-150, 2011.
- [12] R. J. Jaszczak, J. Li, H. Wang, M. R. Zalutsky, and R. E. Goleman, "Pinhole collimation for ultra-high-resolution, small-field-of-view SPECT," *Phys. Med. Biol.*, vol. 39, pp. 425-437, 1994.
- [13] K. Ogawa, T. Kawade, K. Nakamura, A. Kubo, and T. Ichihara, "Ultra high resolution pinhole SPECT for small animal study," *IEEE Trans. Nucl. Sci.*, vol. 45, pp. 3122-3126, 1998.

- [14] S. Jan, D. Benoit, E. Becheva, T. Carlier, F. Cassol, P. Descourt, T. Frisson, L. Grevillot, L. Guigues, L. Maigne, C. Morel, Y. Perrot, N. Rehfeld, D. Sarrut, D. R. Schaart, S. Stute, U. Pietrzyk, D. Visvikis, N. Zahra, and I. Buvat, "GATE V6: a major enhancement of the GATE simulation platform enabling modelling of CT and radiotherapy," *Phys. Med. Biol.*, vol. 56, pp. 881-901, 2011.
- [15] A. Konik, M. T. Madsen, and J. J. Sunderland, "GATE simulations of small animal SPECT for determination of scatter fraction as a function of object size," *IEEE Trans. Nucl. Sci.*, vol. 59, pp. 1887-1891, 2012.
- [16] S. Stute, T. Carlier, K. Cristina, C. Noblet, A. Martineau, B. Hutton, L. Barnnden, and I. Buvat, "Monte Carlo simulations of clinical PET and SPECT scans: impact of the input data on the simulated images," *Phys. Med. Biol.*, vol. 56, pp. 6441-6457, 2011.
- [17] D. Lazaro, I. Buvat, G. Loudos, D. Strul, G. Santin, N. Giokaris, D. Donnarieix, L. Maigne, V. Spanoudaki, S. Styliaris, S. Staelens, and V. Breton," *Phys. Med. Biol.*, vol. 49, pp. 271-285, 2004.
- [18] D. Bollini, A. E. Cabal Rodriguez, W. Dabrowski, A. D. Garcia, M. Gambaccini, P. Giubellino, P. Grybos, M. Idzik, A. Marzari-Chiesa, L. M. Montano, F. Prino, L. Ramello, M. Sitta, K. Swientek, R. Wheadon, and P. Wiacek, "Energy resolution of a silicon detector with the RX64 ASIC designed for X-ray imaging," *Nucl. Instrum. Meth. Phys. Res.*, vol. 515, pp. 458-466, 2003.
- [19] M. Singh and C. Horne, "Use of a germanium detector to optimize scatter correction in SPECT," *J. Nucl. Med.*, vol. 28, pp. 1853-1860, 1987.
- [20] T. Takahashi and S. Watanabe, "Recent progress in CdTe and CdZnTe detectors," *IEEE Trans. Nucl. Sci.*, vol. 48, pp. 950-959, 2001.
- [21] J. Xu, S. Miyazaki, and M. Hirose, "High-quality hydrogenated amorphous silicon-germanium alloys for narrow bandgap thin film solar cells," *J. Non-Crys. Solids*, vol. 208, pp. 277-281, 1996.
- [22] S. D. Sordo, L. Abbene, E. Caroli, A. M. Mancini, A. Zappettini, and P. Ubertini, "Progress in the development of CdTe and CdZnTe semiconductor radiation detectors for astrophysical and medical applications," *Sensors*, vol. 9, pp. 3491-3526, 2009.
- [23] C. Scheiber, "CdTe and CdZnTe detectors in nuclear medicine," *Nucl. Instrum. Meth. Phys. Res.*, vol. 448, pp. 513-524, 2000.
- [24] H. Toyokawa, Y. Furukawa, T. Hirono, H. Ikeda, K. Kajiwara, M. Kawase, T. Ohata, G. Sato, M. Sato, T. Takahashi, H. Tanida, T. Uruga, and S. Watanabe, "Si and CdTe pixel detector developments at Spring-8," *Nucl. Instrum. Meth. Phys. Res.*, vol. 636, pp. S218-S221, 2011.
- [25] Y.-J. Lee and H.-J. Kim, "Comparison of a newly-designed stack-up collimator with conventional parallel-hole collimators in pre-clinical CZT gamma camera systems: a Monte Carlo simulation study," *J. Kor. Phys. Soc.*, vol. 65, pp. 1149-1158, 2014.